This article has been accepted for inclusion in a future issue of this journal. Content is final as presented, with the exception of pagination.

An Enhanced Model Predictive Torque Control With Online Loss Minimization Tracking for SPMSM Drive

Sunbo Wang, Marco Rivera, *Senior Member, IEEE*, Chris Gerada, *Senior Member, IEEE*, Patrick Wheeler, *Fellow, IEEE*, and Neophytos Lophitis

***Abstract*—Maximum efficiency per ampere (MEPA) control, also known as loss minimization (LM) control, aims to minimize losses in permanent magnet synchronous machine (PMSM) drive systems by optimizing the *dq*-axis current references. Addressing the complexities associated with precise drive loss models and the challenges of implementing online optimization for MEPA/LM, this article introduces an enhanced model predictive torque control (MPTC). This new strategy incorporates a reformulated cost function that integrates LM control within the conventional MPTC framework, treating it as a constrained optimization problem. The stability of the proposed MPTC approach is theoretically analyzed using Lyapunov stability theory. Simulation and experimental results validate the control accuracy, dynamic response, and efficiency gains facilitated by this innovative strategy.**

***Index Terms*—Loss minimization (LM) control, model predictive torque control (MPTC), permanent magnet synchronous machine (PMSM).**

I. Introduction

As global efforts intensify to achieve "net zero" and combat climate change, the transportation industry's irreversible move towards electrification continues to gain momentum [1].

Received 22 June 2024; revised 3 October 2024; accepted 26 October 2024. This work was supported in part by the Agencia Nacional de Investigación y Desarrollo (ANID) FONDECYT Regular under Grant 1220556, in part by the ANID under Grant FOVI230169, in part by Fondap SERC under Grant 1523A0006, and in part by the Research Project PINV01-743 of the Consejo Nacional de Ciencia y Tecnología (CONACYT) under Grant ENNOBLE-R02401 and Grant IRCF 24932270 project from the University of Nottingham. *(Corresponding author: Sunbo Wang.)*

Sunbo Wang, Chris Gerada, and Patrick Wheeler are with the Department of Electrical and Electronic Engineering, Faculty of Engineering, Power Electronics, Machines and Control (PEMC) Research Institute, University of Nottingham, NG7 2GT Nottingham, U.K. (e-mail: sunbo.wang@nottingham.ac.uk; eezcg@exmail.nottingham.ac.uk; pat.wheeler@nottingham.ac.uk).

Marco Rivera is with the Department of Electrical and Electronic Engineering, Faculty of Engineering, Power Electronics, Machines and Control (PEMC) Research Institute, University of Nottingham, NG7 2GT Nottingham, U.K., and also with the Laboratorio de Conversión de Energías y Electrónica de Potencia (LCEEP), Vicerrectoría Académica, Universidad de Talca, Talca 3460000, Chile (e-mail: marco.rivera@nottingham.ac.uk; marcoriv@utalca.cl).

Neophytos Lophitis is with the Cyprus University of Technology, Limassol 3036, Cyprus, and also with the University of Nottingham, NG7 2GT Nottingham, U.K. (email: neophytos.lophitis@cut.ac.cy; neo.lophitis1@nottingham.ac.uk).

Digital Object Identifier 10.1109/TIE.2024.3493173

Permanent magnet synchronous machines (PMSMs) are emerging as a particularly attractive technology due to their high-power density, high efficiency, and broad operational range [2], [3], [4]. Advanced control strategies are essential to fully leverage this intrinsic efficiency, which contributes to longer travel distances per charge and reduced energy consumption from batteries [5].

In existing literature, motor efficiency enhancement strategies are primarily categorized into maximum torque per ampere (MTPA) [6], [7], [8] and maximum efficiency per ampere or loss minimization (MEPA/LM) approaches [9], [10], [11], [12], [13], [14], [15], [16], [17], [18], [19]. MTPA control focuses on optimizing torque relative to source current by deriving optimal dq-axis current references through parameter-based methods or online search strategies [6], [7], [8]. However, this control primarily targets copper loss minimization, necessitating further considerations for iron loss and machine drive loss, especially at higher speeds or light loads.

MEPA/LM methods strive for optimal efficiency or minimal power loss, divided into loss model-based and online searching strategies. Loss model-based methods depend on accurate machine loss models to determine optimal dq-axis current references [9], [10], [11], [12], [13]. These methods are capable of accounting for various types of losses, including drive losses [14], but they come with the significant drawback of high computational complexity and extended processing times due to the necessity for detailed finite element analysis (FEA) simulations or exhaustive experimental procedures for precise nonlinear loss characterization [15]. The absence of analytical solutions for these complex models often necessitates the use of lookup tables or high-order polynomial approximations [9], [11], [12], which can heavily burden the memory resources of real-time controllers.

To address these limitations, online searching algorithms have been developed to offer greater flexibility and adaptability. These algorithms dynamically obtain the optimal reference from the loss model in real-time, effectively reducing sensitivity to parameter variations. This flexibility is often achieved by combining the search process with online parameter estimation techniques, as discussed in [16], [17]. The typical operation of these algorithms involves iteratively updating the current reference to minimize power loss through the following steps: 1) calculating the efficiency gradient (or an equivalent method),

2) adjusting the stator current vector to reduce the gradient, and 3) stopping once the gradient nears zero. This process generally involves virtual updates to the loss model [18], [19] or the injection of small signals [20]. However, these algorithms often require multiple control intervals to converge, which can detract from the system's responsiveness.

Finite-set model predictive torque control (FS-MPTC) and finite-set model predictive current control (FS-MPCC) have emerged as robust control strategies due to their inherent compatibility with the discrete operation of power converters and superior transient performance [21]. These FS-MPC strategies can be employed as inner loops in conjunction with traditional LM methods, whether online or offline [22], [23]. However, existing FS-MPC-based LM methods often inherit the drawbacks of traditional LM approaches, such as delayed response in tracking the minimum loss point or high demands on computational and storage resources. FS-MPTC's versatile control capabilities uniquely position it to address multiple optimization objectives simultaneously [24]. By integrating the loss minimization goal directly into the cost function, FS-MPTC can achieve online loss optimization, thereby eliminating the need for separate algorithms or additional lookup tables typically associated with MEPA/LM strategies. This integrated approach consolidates reference calculation and current regulation into a single streamlined operation, inherently enhancing dynamic response. Additionally, by calculating only the cost function at each sampling period and carefully designing its structure, the computational load is minimized.

In this article, an enhanced model predictive control strategy that integrates online loss minimization tracking within the cost function is proposed, drawning from the mathematical and loss models of the PMSM drive. The design of the cost function is optimized to improve robustness and tracking accuracy. Simulation and experimental results are presented to validate the theoretical analysis and demonstrate the effectiveness of the proposed method.

II. Mathematics Model and Loss Model of PMSM Drive System

A. PMSM Mathematical Model

Due to saturation and cross-saturation effects there is a strongly nonlinear relationship between the flux linkage and the current. The full order dq-axis current differential equation of PMSMs can be described as follows [13]:

$$\mathbf{L}_{dq}\frac{d\mathbf{i}_{dq}}{dt} = \mathbf{u}_{dq} - R_s\mathbf{i}_{dq} + \boldsymbol{\omega}\boldsymbol{\psi}_{dq} \tag{1}$$

here, $\mathbf{i}_{dq} = \begin{bmatrix} i_d & i_q \end{bmatrix}^T$ represents the stator currents, $\boldsymbol{\psi}_{dq} = \begin{bmatrix} \psi_d(\mathbf{i}_{dq}) & \psi_q(\mathbf{i}_{dq}) \end{bmatrix}^T$ represents the flux linkage, $\mathbf{u}_{dq} = \begin{bmatrix} u_d & u_q \end{bmatrix}^T$ represents the stator voltages, R_s represents the phase resistance, $\boldsymbol{\omega} = \begin{bmatrix} 0 & \omega \\ -\omega & 0 \end{bmatrix}$ represents the matrix of electrical angular velocity ω, and the inductance matrix $\mathbf{L}_{dq}$ is defined as

$$\mathbf{L}_{dq}(\mathbf{i}_{dq}) = \begin{bmatrix} L_{dd}(\mathbf{i}_{dq}) & M_{dq}(\mathbf{i}_{dq}) \\ M_{qd}(\mathbf{i}_{dq}) & L_{qq}(\mathbf{i}_{dq}) \end{bmatrix} = \begin{bmatrix} \dfrac{\partial\psi_d}{\partial i_d} & \dfrac{\partial\psi_d}{\partial i_q} \\ \dfrac{\partial\psi_q}{\partial i_d} & \dfrac{\partial\psi_q}{\partial i_q} \end{bmatrix}. \tag{2}$$

The electromagnetic torque is described by

$$T_{\text{em}} = \frac{3}{2}p(\psi_d i_q - \psi_q i_d). \tag{3}$$

To predict the torque and minimize losses in the PMSM drive system, the dq-axis currents at the $(k+1)th$ instant are determined by discretizing (1) using the Taylor method

$$\begin{aligned}\mathbf{i}_{dq}(k+1) = (\mathbf{I} - \mathbf{L}_{dq}^{-1}R_s)\mathbf{i}_{dq}(k)T_s \\ + \mathbf{L}_{dq}^{-1}\mathbf{u}_{dq}(k)T_s + \mathbf{L}_{dq}^{-1}\boldsymbol{\omega}(k)\boldsymbol{\psi}_{dq}(k)\end{aligned} \tag{4}$$

where T_s denotes the sampling period of the controller.

B. PMSM Drive System Loss Model

The PMSM losses comprise copper loss, iron loss, mechanical loss, and other additional losses [25]. Mechanical and additional losses, typically minor and noncontrollable, are neglected in efficiency optimization.

The dc phase resistance is generally measured when the motor is stationary, which can represent dc copper loss. When PMSMs operate with high speed and high fundamental frequency, the ac copper loss is so large that can not be neglected. The total copper loss is obtained as

$$P_{\text{cu}} = \frac{3}{2}(R_{\text{dc}} + R_{\text{ac}})(i_d^2 + i_q^2) \tag{5}$$

where R_{dc} is the dc resistance, and R_{ac}, factoring in the eddy effect, is a frequency-dependent ac resistance modeled as

$$R_{\text{AC}} = R_{\text{DC}}(K_I f + K_{II} f^2). \tag{6}$$

Iron loss, commonly modeled by Steinmetz's equation [15], is separated into hysteresis and eddy current losses

$$dP_{\text{Fe}} = K_h f_m B_p^{\alpha} + K_e f_m^2 B_p^2. \tag{7}$$

dP_{Fe} denotes the iron loss per unit volume, K_h and K_e are the coefficients for hysteresis and eddy current losses, respectively, f_m is the fundamental frequency, and B_p is the peak magnetic flux density.

The total iron loss is obtained by by summing the dP_{Fe} across all meshed elements, including the stator tooth and stator yoke, which is expressed as

$$P_{\text{Fe}} = dP_{\text{Fe},T}V_T + dP_{\text{Fe},Y}V_Y \tag{8}$$

where V_T and V_Y are the volume of stator tooth and yoke, respectively. Assuming the flux density is uniformly distributed within the stator tooth and yoke, the flux densities in the tooth B_T and in the yoke B_Y are derived from dq-axis fluxes as

$$\begin{cases} B_T &= \dfrac{\sqrt{\psi_d^2+\psi_q^2}}{N_1 A_T} \\ B_Y &= \dfrac{\sqrt{\psi_d^2+\psi_q^2}}{N_1 A_Y} \end{cases} \tag{9}$$

where N_1 is the number of turns per phase, A_T and A_Y are the equivalent cross-sectional areas of the stator tooth and yoke, respectively.

The total stator iron loss can then be derived from (7) to (9) as follows [13]:

$$\begin{cases} P_{\text{Fe}} = K_{hs} f_m (\psi_d^2+\psi_q^2)^{\alpha/2} + K_{es} f_m^2 (\psi_d^2+\psi_q^2) \\ K_{hs} = K_h \left(\dfrac{V_T}{N_1^\alpha A_T^\alpha} + \dfrac{V_Y}{N_1^\alpha A_Y^\alpha} \right) \\ K_{es} = K_e \left(\dfrac{V_T}{N_1^2 A_T^2} + \dfrac{V_Y}{N_1^2 A_Y^2} \right). \end{cases} \tag{10}$$

The inverter loss consists of conduction and switching losses. Conduction loss, related to the on-resistance of devices and dq-axis currents, is given by

$$P_{\text{con}} = \frac{3}{2} R_{\text{on}} (i_d^2 + i_q^2). \tag{11}$$

Switching loss, inherently nonlinear, can be first estimated by determining the turnon and turnoff energies using analytical models or experimental methods [26]. Under the empirical assumption of constant turnoff voltages and efficient cooling, the switching energy is approximated by a polynomial function of the conduction current i_{con}:

$$E_{\text{sw}}(i_L) = E_{\text{on}}(i_{\text{con}}) + E_{\text{off}}(i_{\text{con}}) = \sum_{n=0}^{N} K_n i_L^n + o. \tag{12}$$

K_n are the coefficients of the polynomial fit, and o is an infinitesimal term, negligible in calculations. The switching loss for the inverter is then calculated by integrating the switching energy over one fundamental period

$$\begin{aligned} P_{sw} &= 3 \cdot \frac{2 f_{sw}}{f_F} \int_0^{1/f_F} \left(\sum_{n=0}^{N} K_n (i_s \cos \omega t)^n + o \right) dt \\ &= f_{sw} (K_{sw,0} + K_{sw,1} i_s + K_{sw,2} i_s^2 + \ldots) \end{aligned} \tag{13}$$

f_F is the fundamental frequency, f_{sw} is the switching frequency, and i_s is the phase current amplitude, with $i_s = \sqrt{i_d^2 + i_q^2}$. $K_{sw,i}$ are the fitting coefficients in proportional to K_n. The switching frequency of FS-MPC can be variable, and average switching frequency should be applied to compute the average switching times over a time interval to represent the average switching loss [27]

$$f_{\text{sw}} = \frac{1}{3 \cdot 2 N T_s} \sum_{n=1, i=a,b,c}^{N} |S_i(n) - S_i(n-1)|. \tag{14}$$

Consequently, the total loss is

$$P_{\text{loss}} = P_{\text{Cu}} + P_{\text{Fe}} + P_{\text{con}} + P_{sw} \tag{15}$$

with these losses determined, the output torque and PMSM drive system loss for the subsequent instant can be predicted using (5) to (15), based on the discretized model of (4).

III. Proposed FS-MPTC With Online Loss Minimization Tracking

The preceding section detailed a methodology for predicting torque and assessing losses in the PMSM drive system with mathematical model. Intuitively, the optimal control objective should encompass both torque error and power loss within the cost function. However, this introduces a paradox, as increasing torque typically results in inevitably higher power loss, and vice versa, creating intrinsic tracking errors for both control targets. These errors, introduced by conflicting control objectives, can only be balanced rather than eliminated by adjusting the weight factor. Additionally, the complexity of the loss model hinders the identification of an optimized power loss point or the derivation of a corresponding analytical expression as MTPA [28]. To address these issues, a new cost function is proposed that aims to achieve precise torque tracking and power loss minimization, as well releasing the reliance on weight factor selection to enhance the system's robustness.

A. Proposed FS-MPTC Formulation

The proposed FS-MPTC formulation aims to optimize the drive system's efficiency while maintaining the reference torque. The optimization problem for this model predictive control approach can be expressed as minimizing the total power loss P_{loss} given constraints on the desired electromagnetic torque T_{em} and the allowable current bounds

$$\begin{aligned} &\text{minimize} P_{\text{loss}}(i_d, i_q) \\ &\text{subject to } T_{\text{em}}(i_d, i_q) = T_{\text{em}}^* \\ &\qquad i_d \in [i_{d\text{min}}, i_{d\text{max}}] \\ &\qquad i_q \in [i_{q\text{min}}, i_{q\text{max}}]. \end{aligned} \tag{16}$$

Assuming a constant speed for the PMSM, the power loss P_{loss} with the constraint of maintaining the reference torque is shown in Fig. 1. The gradient of the electromagnetic torque, indicated in Fig. 1 as $(\partial T_{\text{em}}/\partial i_d, \partial T_{\text{em}}/\partial i_q)$, points in the direction of the steepest increase in torque. At the reference torque, the system loss initially decreases with an increase in i_d ($dP_{\text{loss}} < 0$), reaching a minimum at the loss minimization (LM) point where $dP_{\text{loss}} = 0$, and then increases as i_d continues to rise ($dP_{\text{loss}} > 0$). To minimize P_{loss} while keeping the torque constant, the trajectory of the dq-axis current pair (i_d, i_q) should follow a contour line perpendicular to the gradient vector, satisfying:

$$(di_d, di_q) = \left(-\frac{\partial T_{\text{em}}}{\partial i_q}, \frac{\partial T_{\text{em}}}{\partial i_d} \right). \tag{17}$$

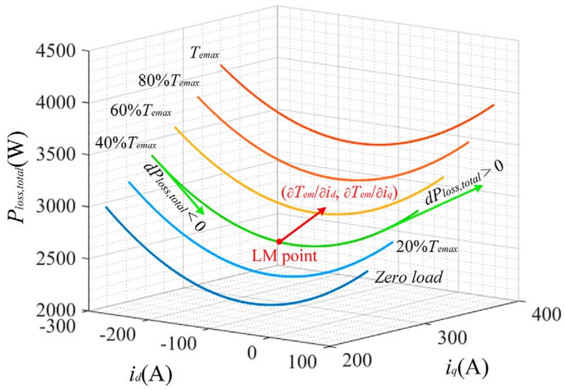

Fig. 1. PMSM drive system loss versus dq-axis current with different constant torques.

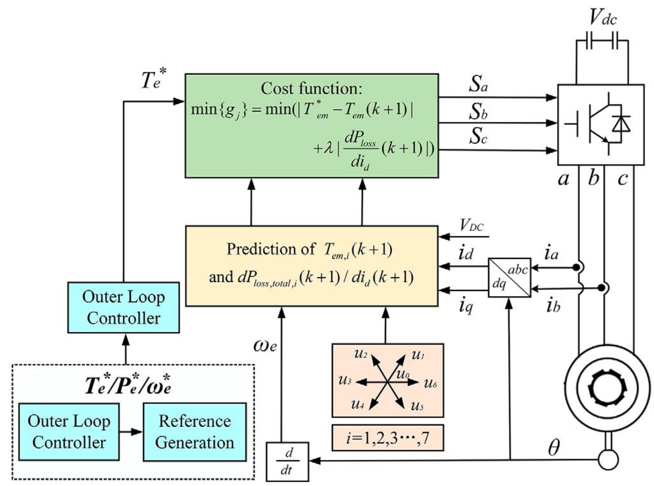

Fig. 2. Proposed enhanced FS-MPTC with loss minimization tracking for PMSM drive system.

Following the contour line, the differential of the total power loss P_{loss} with respect to i_d is calculated as:

$$\frac{dP_{\text{loss}}}{di_d} = -\frac{\partial P_{\text{loss}}}{\partial i_q}\frac{\partial T_{\text{em}}/\partial i_d}{\partial T_{\text{em}}/\partial i_q} + \frac{\partial P_{\text{loss}}}{\partial i_d}. \tag{18}$$

This differential is equivalent to zero at the loss minimization point.

To achieve the minimum drive system loss while meeting the reference torque, the cost function is defined as the absolute value of the torque error $|T^*_{\text{em}} - T^p_{\text{em}}|$ and the derivative of power loss P^p_{loss}, simplified as

$$g = |T^*_{\text{em}}(k+1) - T_{\text{em}}(k+1)| + \lambda\left|\frac{dP_{\text{loss}}}{di_d}(k+1)\right|. \tag{19}$$

T^*_{em} is the reference torque from the speed or power control loop, $T_{\text{em}}(k+1)$ is the predicted torque for the $(k+1)$th instant as determined by (3) and (4), $(dP_{\text{loss}}/di_d)(k+1)$ is the predicted rate of change in power loss following the constant torque direction for the next instant, as described by (4) and (18), and λ is the weighting factor. The block diagram for the proposed FS-MPTC with loss minimization tracking is shown in Fig. 2. Unlike the cost functions of FS-MPTC discussed in [22] and [28], which also incorporate current/loss minimization tracking, the proposed method replaces the stator flux control component with an absolute value that reflects proximity to the minimum loss point. This approach allows the proposed FS-MPTC method to inherently track the minimum loss point while simultaneously achieving the desired torque, eliminating the execution delay typically associated with the outer loss minimization control loop found in conventional methods. From the cost function in (19), it's evident that the Euclidean distance, projected perpendicular to the torque gradient, is utilized for the loss minimization part of the cost function, while the distance along the gradient direction is used for the torque component. These are almost decoupled, similar to FS-MPCC. Thus, following FS-MPCC principles, the most direct trajectory should be taken from the current state to the desired state.

B. Stability of the Proposed FS-MPTC

The stability of the proposed FS-MPTC is affirmed through Lyapunov stability theory. Consider a Lyapunov function derived from the desired torque error and desired loss point error

$$V(x_1, x_2) = \frac{1}{2}m_1 x_1^2 + \frac{1}{2}m_2 x_2^2 \tag{20}$$

where m_1, m_2 are the coefficient, x_1 symbolizes the torque error component from the cost function, and x_2 represents the proximity to the minimum loss point from the cost function in (19), expressed as

$$x_1 = T_{\text{em}} - T^*_{\text{em}} \tag{21}$$

$$x_2 = \frac{dP_{\text{loss}}}{di_d}. \tag{22}$$

The derivative of (20) with respect to time is obtained as

$$\begin{aligned}\dot{V}(x_1, x_2) &= m_1\dot{x}_1 x_1 + m_2\dot{x}_2 x_2 \\ &= K_1\frac{di_d}{dt} + K_2\frac{di_q}{dt}\end{aligned} \tag{23}$$

where K_1 and K_2 are coefficients derived from the differential formulae of T_{em} and P_{loss} in (3) and (18) as

$$\begin{cases} K_1 = m_1(T_{\text{em}} - T^*_{\text{em}})\dfrac{\partial T_{\text{em}}}{\partial i_d} + m_2\dfrac{(\partial dP_{\text{loss}}/di_d)}{\partial i_d} \\ K_2 = m_2(T_{\text{em}} - T^*_{\text{em}})\dfrac{\partial T_{\text{em}}}{\partial i_q} + m_2\dfrac{(\partial dP_{\text{loss}}/di_d)}{\partial i_q}. \end{cases} \tag{24}$$

Given that the machine source voltage remains within the voltage vectors hexagon and the PMSM drive operates within the linear modulation zone, there will always exist dq-axis control voltages (u_d, u_q) that render the dq-axis current derivative vector $(di_d/dt, di_q/dt)$ obtuse to the coefficient vector (K_1, K_2) and fulfill

$$\dot{V}(x_1, x_2) = (K_1, K_2)\cdot\left(\frac{di_d}{dt}, \frac{di_q}{dt}\right) < 0. \tag{25}$$

TABLE I
PARAMETER OF THE PROTOTYPE SPMSM

Parameters	Values	Parameters	Values
Number of poles	10	Rated current (A)	750
Number of slots	12	Phase resistance R_s (mΩ)	4.7
Rated power (kW)	250	PM flux linkage (Wb)	0.0506
Base speed (r/min)	7000	Stator inductance L (μH)	72

Consequently, a local control law with a control sequence $[u_1, u_2, \ldots, u_K]$ exists within the proposed cost function in (19) that leads to $g(n+K) < \varepsilon$, where ε is a small positive value indicating the boundary. Thus, the proposed FS-MPTC with loss minimization tracking is asymptotically stable. It's noteworthy that the asymptotic stability is not influenced by the weight factor λ, which corresponds to the coefficient in the Lyapunov function.

When the control sequence $[u_1, u_2, \ldots, u_K]$ is sufficiently extensive and the sampling period sufficiently small, the cost function $g(n+K)$ reaches zero, and

$$\begin{cases} |T_{\text{em}} - T_{\text{em}}^*| \to 0 \\ \left|\dfrac{dP_{\text{loss}}}{di_d}\right| \to 0. \end{cases} \tag{26}$$

For the loss minimization problem introduced in (16), the general solution can be derived using the Lagrange method [13]. The Lagrangian function is defined as

$$\mathcal{L}(i_d, i_q, \lambda_L) = P_{\text{loss}}(i_d, i_q) + \lambda_L \left(T_{\text{em}}(i_d, i_q) - T_{\text{em}}^*\right) \tag{27}$$

where λ_L is the Lagrange multiplier. When λ_L satisfies

$$\lambda_L = -\frac{\partial P_{\text{loss}}/\partial i_q}{\partial T_{\text{em}}/\partial i_q} \tag{28}$$

the following conditions are satisfied under the constraints defined in (26):

$$\begin{cases} \dfrac{\partial \mathcal{L}}{\partial i_d} \to 0 \\ \dfrac{\partial \mathcal{L}}{\partial i_q} \to 0 \\ \dfrac{\partial \mathcal{L}}{\partial \lambda_L} \to 0. \end{cases} \tag{29}$$

The conditions in (29) correspond to the solution of the original constrained optimization problem with Lagrange method. Therefore, the proposed FS-MPTC strategy theoretically achieves the desired torque and minimum loss point with a sufficiently long control sequence, provided the sampling period is small enough. This ensures that the tracking of the desired torque and the minimization of losses are simultaneously attained in the steady state.

IV. Simulation and Experiment Validation

The proposed FS-MPTC was validated on a 220 kW PMSM drive system, detailed in Table I. The experimental setup, carried out on a test bench depicted in Fig. 3, includes a three-phase inverter composed of SiC MOSFETs, as detailed in Table II, and managed by an ARM+FPGA controller. The dynamometer shown in Fig. 3 served as a speed load, with the prototype drive system operating in torque mode.

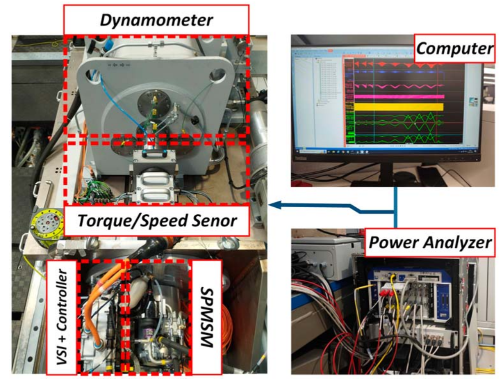

Fig. 3. Experimental testing platform.

TABLE II
TECHNICAL DATA FOR SiC MOSFET MODULE AT TEMPERATURE 25 °C

Variables	Values
Switching threshold voltage (V)	2.12
Diode threshold voltage (V)	1.67
Switching conduction resistance (mΩ)	1.1
Input capacitance @ $V_{DS} = 800$V (nF)	79.4
Turn on energy E_{on} @$V_{DS} = 600$V, $I_{DS} = 760$A (mJ)	20.3
Turn off energy E_{off} @$V_{DS} = 600$V, $I_{DS} = 760$A (mJ)	17.9

The controller's sampling frequency was set to 25 μs, incorporating a 1 μs dead time to avoid simultaneous conduction during the switching of each phase. The dc-link voltage was maintained at 750 V. The weighting factor are emperically set at $|T_{\text{emax}}/(dP_{\text{loss}}/di_d)_{\max}|$, to balance LM point tracking and desired torque tracking effectively.

According to prior research, FS-MPCC or FS-MPTC methods with a prebuilt look-up table can achieve rapid dynamic performance in LM point tracking, though constructing such a table demands significant computational effort. To evaluate dynamic and steady-state performance, both the FS-MPTC+LM method from [23] and the proposed FS-MPTC strategy were independently implemented in simulations and experiments. For the FS-MPTC+LM method, the weighting factor was selected as $|T_{\text{emax}}/\psi_{\max}|$. Importantly, the FS-MPTC+LM method requires an additional 100×100 look-up table, alongside the stator inductance map and loss model coefficients (as listed in Table III), to store optimal stator flux references for minimum loss tracking. This look-up table, occupying 40 kB of storage space in the controller, is an extra requirement that is not necessary in the proposed FS-MPTC method.

The ac current waveforms were measured using LEM HTFS800 sensors, and the angle data was acquired with a RO3620 resolver, which facilitated the transformation of data

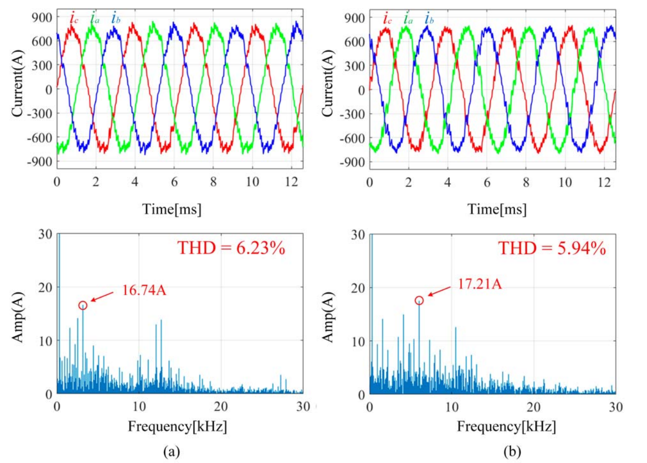

Fig. 4. Steady-state current waveforms and harmonic spectrum at 3000 rpm and 260 Nm. (a) Steady-state phase currents waveforms for MPTC+LMC. (b) Steady-state phase currents waveforms for proposed MPTC.

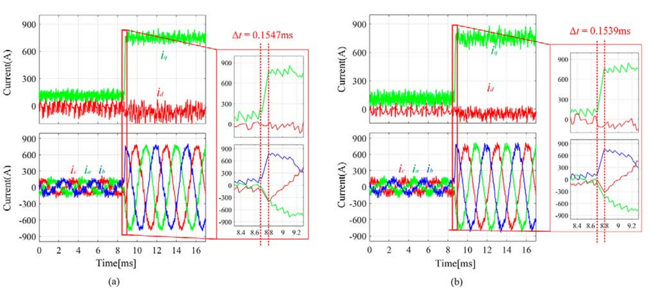

Fig. 5. Torque dynamic response as the torque step from 20% to 100%. (a) MPTC+LMC. (b) Proposed MPTC.

into the dq-axis. The speed and torque were measured using an HBM T40B sensor, while the dc voltage and current were monitored through an HBM GN310B card. The efficiency and loss performance of the drive system were analyzed using an HBM power analyzer, where losses were calculated from the difference between the dc input power and the mechanical output power. The total measurement error was maintained within 0.015% of the rated power, or $\pm$45 W.

A. Simulation Tests

The PLECS simulation environment replicates the experiment platform to validate the proposed MPTC method, utilizing the actual system parameters. Under a constant speed of 3000 rpm and a load of 260 Nm, the steady-state currents and phase current spectrum are presented in Fig. 4. It is indicated that the steady-state performance of the proposed FS-MPTC aligns closely with that of the FS-MPTC+LM, even showing slight improvements in current harmonics in certain respects.

Keeping the same rotational speed and an abrupt torque reference shift from 20% to full load, the dynamic behavior of the proposed FS-MPTC is compared with the conventional FS-MPTC+LM as shown in Fig. 5. The transition time for both MPTC strategies is observed to be around 150 μs, equivalent

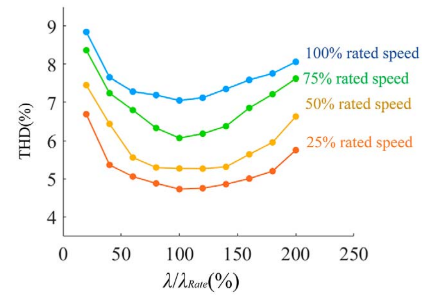

Fig. 6. THD versus weighting factor of nominal at different load.

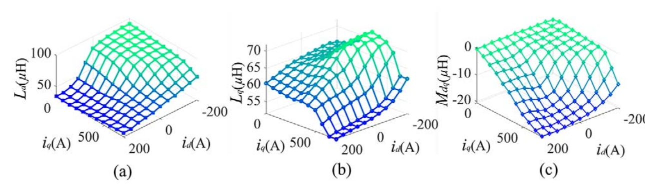

Fig. 7. Stator inductances under various dq-axis current conditions. (a) d-axis inductance. (b) q-axis inductance. (c) dq-axis mutual inductance.

to approximately six sampling periods. This suggests that, in contrast to traditional MPTC strategies which employ desired flux as a secondary cost function component, the proposed MPTC does not elongate the tracking intervals to the desired operational point, thereby maintaining equivalent dynamic performance.

Fig. 6 evaluates the sensitivity of the proposed method to the weighting factor, demonstrating stability with it across a broad range from 20% to 200% of nominal values. The total harmonic distortion (THD) reaches a minimum near the rated value. This corresponds with the empirical design, and suggests a weak dependence on the weighting factor selection and a strong robustness of the proposed FS-MPTC strategy.

B. Experimental Tests

The accuracy of the proposed loss model is highly dependent on the precision of the machine parameters. Similarly, the effectiveness of model predictive control is contingent upon accurate machine parameter inputs. To achieve this, finite element analysis (FEA) was employed to determine the stator's inductance values under various dq-axis current conditions. These inductance measurements, depicted in Fig. 7, provide a reliable estimation of the machine parameters essential for the LM tracking and MPTC strategies.

Fig. 8 presents a comparison between the predicted losses using the proposed FS-MPTC strategy and experimental measurements across varying loads and rotational speeds. The coefficients used to predict the losses, which are derived from the datasheets of winding litz wires, stator materials, and SiC MOSFETs, are listed in Table III. The Normalized Root Mean Square Error (NRMSE) between the predicted and measured losses of the SPMSM drive system is calculated to be below 5%, confirming the accuracy of the loss model for application in the online optimal algorithm.

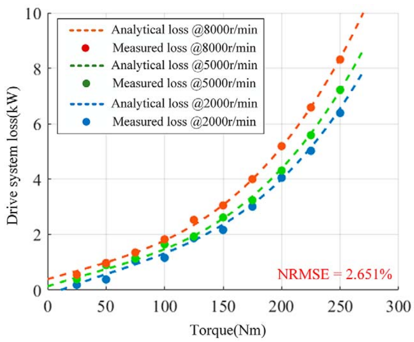

Fig. 8. Comparison of the PMSM drive system loss with proposed loss model estimation and measurement results.

TABLE III
COEFFICIENTS OF THE PMSM DRIVE SYSTEM LOSS MODEL

Coefficients	Values	Coefficients	Values
K_{hs}	361.344	K_I	2.2442e-5
K_{es}	1.8	K_{II}	8.6293e-8
$K_{sw,0}$	9.764e-3	$K_{sw,1}$	1.048e-4
$K_{sw,2}$	9.993e-08		

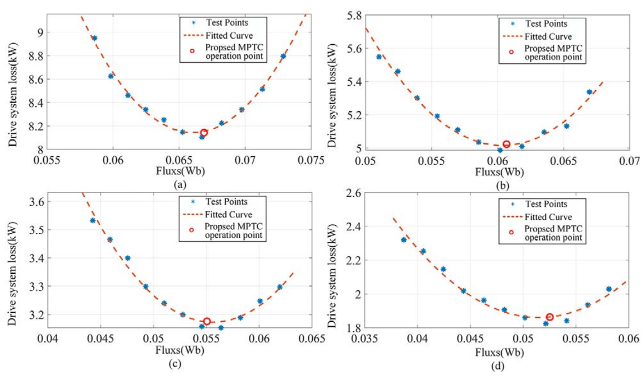

Fig. 9. Stator flux sweep test results with different load at 8000 r/min. (a) Torque260Nm. (b) Torque200Nm. (c) Torque140Nm. (d) Torque80Nm.

The steady-state performance of the proposed MPTC is evaluated from two perspectives: 1) the accuracy of loss minimization tracking; 2) the quality of the phase current waveform. Fig. 9 demonstrates the tracking accuracy of the loss minimization point with the proposed MPTC strategy. In this test, a traditional MPTC is applied, and the stator flux reference sweeps from minimum to maximum. This test is repeated under different load conditions, identifying the optimal stator flux at the valley of the loss fitting curve. This result is compared with the observed stator flux using the proposed MPTC strategy, as detailed in Table IV. The discrepancy, not exceeding 1.5%, confirms that the proposed MPTC strategy can accurately track the optimal operating point with respect to efficiency. The steady-state currents were comparatively measured under full load at 5000 r/min between the proposed FS-MPTC and FS-MPTC+LM and are presented in Fig. 10. The spectrum

TABLE IV
COMPARISON BETWEEN THE OBSERVATION OF STATOR FLUX WITH PROPOSED MPTC STRATEGY AND DETECTED RESULTS

Torque(Nm)	80	140	200	260
Detected stator flux(Wb)	0.0521	0.0561	0.0611	0.0669
Observed stator flux(Wb)	0.0527	0.0553	0.0607	0.0676
Error (%)	1.14	1.26	0.65	1.04

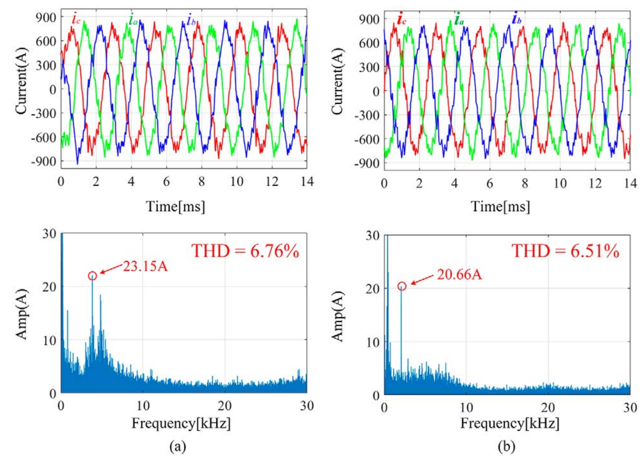

Fig. 10. Steady state phase currents waveform at full load, 5000 r/min. (a) Steady-state phase currents waveforms for MPTC+LMC. (b) Steady-state phase currents waveforms for proposed MPTC.

analysis of the phase currents reveals that the proposed FS-MPTC achieves a 13% reduction in peak current harmonics and a 0.25% reduction in THD with both applying the empirical weighting factors.

The dynamic performance of the proposed MPTC strategy is validated through the results in Figs. 11 and 12. Fig.11 shows the dq-axis currents and phase currents both before and after the activation of the proposed FS-MPTC strategy. Initially, the traditional MPTC strategy is applied, with stator flux reference is set to MTPA operation point. Upon activation of the proposed method, the cost function is modified to (19), enable the minimization loss traction. The dq-axis currents stabilize approximately two sampling periods after the proposed method's activation, demonstrating the superior dynamic performance of the proposed FS-MPTC strategy with loss minimization tracking capability.

Among the existing research, FS-MPTC+LM or FS-MPCC+LM strategy with prebuilt look-up tables provides the best dynamic response, but albeit at the cost of high computational burdens and data storage requirements. As shown in Fig. 12, when the torque reference is set abruptly increase from 10% of rated load to 100%, the sensitivity and rapidity of load dynamic response of the proposed FS-MPTC strategy are comparable to those of tradition FS-MPTC+LM strategy with look-up table. The settling time for the proposed MPTC strategy is approximately seven sampling periods, which is comparable or even slightly better than that of the conventional MPTC+LM strategy.

In contrast to other online LM methods, which are typically integrated as an outer loop for torque and flux control,

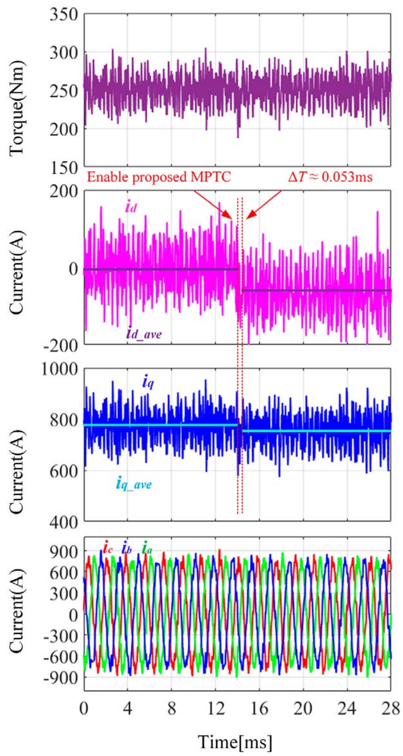

Fig. 11. Minimization loss tracking test of proposed MPTC strategy at rated load, base speed.

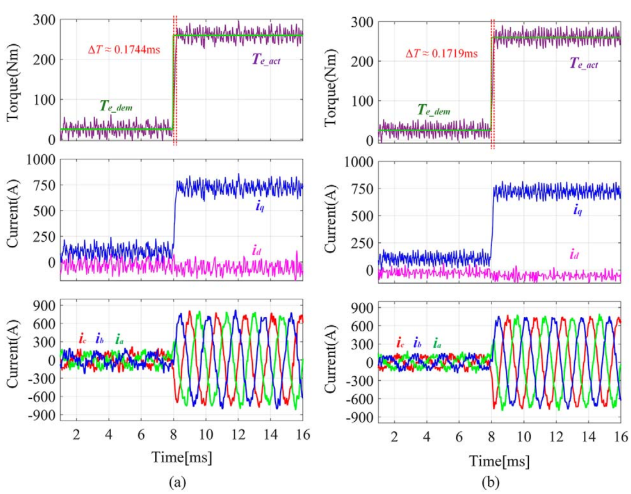

Fig. 12. Step load from 10% of rated load to 100% at base speed. (a) MPTC+LMC. (b) Proposed MPTC.

TABLE V
COMPARISON OF SETTLING DOWN TIME FOR THE STEP LOAD TEST IN FIG. 12

Strategy	Settling Down Time (ms)
Proposed MPTC	0.1719
MPTC + Online LM in [22]	2.745
MPTC + Online LM in [20]	17.641

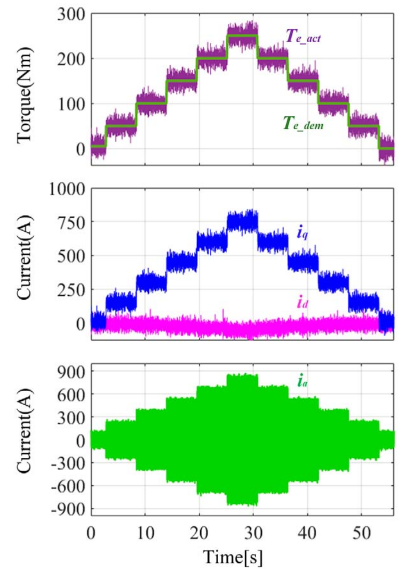

Fig. 13. Measured results of the proposed MPTC strategy at based speed with various load conditions.

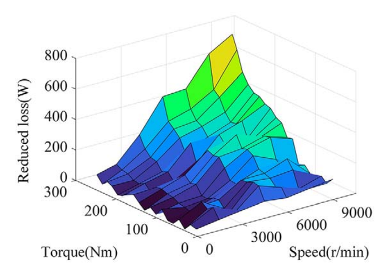

Fig. 14. Measured loss reduction of the proposed MPTC strategy compared with conventional MPTC+MTPA strategy.

the proposed MPTC strategy dynamically tracks the minimum loss point simultaneously with torque control, eliminating the delay associated with outer loop processing. Table V shows the settling times of dq-axis currents for different LM methods under the same step load test as in Fig. 12. It is evident that the proposed MPTC strategy significantly reduces the response delay for minimum loss tracking compared to existing online searching methods such as those in [20] and [22].

To demonstrate the efficiency improvements afforded by the proposed FS-MPTC strategy, a comparison is made with the conventional FS-MPTC+MTPA strategy on the prototype drive system. The stair torque references are swept at various speeds, as illustrated in Fig. 13. The resulting performance of the two strategies on the prototype system is shown in Fig. 14. At lower speeds and torques, the loss reduction offered by the proposed method compared to FS-MPTC+MTPA is minimal. However, as the load increases, the efficiency gains become more pronounced. These gains are attributed to core saturation, where applying reduced d-axis stator flux lessens the current magnitude required for the same torque output. Additionally, at higher speeds, reducing the d-axis flux significantly lowers iron eddy current and hysteresis losses. The enhanced efficiency achieved through the proposed scheme is shown in Fig. 15, where it is evident that the drive system's efficiency exceeds 96% across a wide operational range when this control strategy is implemented.

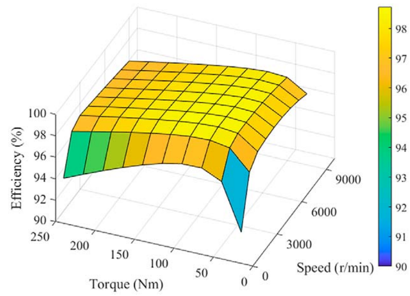

Fig. 15. Drive system efficiency with proposed MPTC strategy under various conditions.

V. Conclusion

This article has introduced an enhanced FS-MPTC strategy capable of online loss minimization tracking in PMSM drive systems. Utilizing the MPC cost function's capacity for multiple objective optimization, a novel cost function formula was developed. Loss minimization control is streamlined as a single-variable problem integrated directly into the cost function, enhancing system efficiency without compromising torque output. The stability of the proposed FS-MPTC is examined using Lyapunov theory, which also underscores the minimal dependency on the weighting factor of the proposed method. Notably, the method does not introduce any ripple or noise into the physical system, thereby preventing additional losses and torque ripple. The method matches the efficacy of offline strategies and eliminates the need for extensive lookup tables. Extensive experimental testing across various operational conditions has validated the accuracy and dynamic performance of the algorithm.

References

[1] T. Zou et al., "A comprehensive design guideline of hairpin windings for high power density electric vehicle traction motors," *IEEE Trans. Transp. Electr.*, vol. 8, no. 3, pp. 3578–3593, Mar. 2022, doi: 10.1109/TTE.2022.3149786.

[2] Q. Wang et al., "A low-complexity optimal switching time-modulated model-predictive control for PMSM with three-level NPC converter," *IEEE Trans. Transp. Electrific.*, vol. 6, no. 3, pp. 1188–1198, Mar. 2020, doi: 10.1109/TTE.2020.3012352.

[3] H. Wang et al., "Three-level indirect matrix converter with neutral-point potential balance scheme for adjustable speed drives," *IEEE Trans. Transp. Electrific.*, vol. 8, no. 1, pp. 845–855, Jan. 2022, doi: 10.1109/TTE.2021.3112536.

[4] F. Guo, T. Yang, C. Li, S. Bozhko, and P. Wheeler, "Active modulation strategy for capacitor voltage balancing of three-level neutral-point-clamped converters in high-speed drives," *IEEE Trans. Ind. Electron.*, vol. 69, no. 3, pp. 2276–2287, Mar. 2022, doi: 10.1109/TIE.2021.3065605.

[5] K. Li and Y. Wang, "Maximum torque per ampere (MTPA) control for IPMSM drives based on a variable-equivalent-parameter MTPA control law," *IEEE Trans. Power Electron.*, vol. 34, no. 7, pp. 7092–7102, Jul. 2019, doi: 10.1109/TPEL.2018.2877740.

[6] Y. Chen et al., "Improved flux-weakening control of ipmsms based on torque feedforward technique," *IEEE Trans. Power Electron.*, vol. 33, no. 12, pp. 10970–10978, Dec. 2018, doi: 10.1109/TPEL.2018.2810862.

[7] K. Huang, W. Peng, C. Lai, and G. Feng, "Efficient maximum torque per ampere (MTPA) control of interior PMSM using sparse Bayesian based offline data-driven model with online magnet temperature compensation," *IEEE Trans. Power Electron.*, vol. 38, no. 4, pp. 5192–5203, Apr. 2023, doi: 10.1109/TPEL.2022.3230052.

[8] X. Qi, L. Aarniovuori, and W. Cao, "Regularization-theory-based fast torque tracking method for interior permanent magnet synchronous machines," *IEEE Trans. Ind. Electron.*, vol. 70, no. 12, pp. 12113–12123, Dec. 2023, doi: 10.1109/TIE.2023.3237895.

[9] J. Lee, K. Nam, S. Choi, and S. Kwon, "Loss-minimizing control of PMSM with the use of polynomial approximations," *IEEE Trans. Power Electron.*, vol. 24, no. 4, pp. 1071–1082, Apr. 2009, doi: 10.1109/TPEL.2008.2010518.

[10] S. Yamamoto, H. Hirahara, A. Tanaka, T. Ara, and K. Matsuse, "Universal sensorless vector control of induction and permanent-magnet synchronous motors considering equivalent iron loss resistance," *IEEE Trans. Ind. Appl.*, vol. 51, no. 2, pp. 1259–1267, Feb. 2015, doi: 10.1109/TIA.2014.2360962.

[11] H. Zhang, M. Dou, and J. Deng, "Loss-minimization strategy of nonsinusoidal back EMF PMSM in multiple synchronous reference frames," *IEEE Trans. Power Electron.*, vol. 35, no. 8, pp. 8335–8346, Aug. 2020, doi: 10.1109/TPEL.2019.2961689.

[12] J. Hang, H. Wu, S. Ding, Y. Huang, and W. Hua, "Improved loss minimization control for ipmsm using equivalent conversion method," *IEEE Trans. Power Electron.*, vol. 36, no. 2, pp. 1931–1940, Feb. 2021, doi: 10.1109/TPEL.2020.3012018.

[13] R. Ni, D. Xu, G. Wang, L. Ding, G. Zhang, and L. Qu, "Maximum efficiency per ampere control of permanent-magnet synchronous machines," *IEEE Trans. Ind. Electron.*, vol. 62, no. 4, pp. 2135–2143, Apr. 2015, doi: 10.1109/TIE.2014.2354238.

[14] D. Hu, W. Xu, R. Dian, Y. Liu, and J. Zhu, "Loss minimization control of linear induction motor drive for linear metros," *IEEE Trans. Ind. Electron.*, vol. 65, no. 9, pp. 6870–6880, Sep. 2018, doi: 10.1109/TIE.2017.2784343.

[15] H. Zhang, M. Dou, and C. Dang, "Loss-optimization method of permanent-magnet synchronous motor based on precise stator iron loss model," *IEEE J. Emerg. Sel. Topics Power Electron.*, vol. 9, no. 5, pp. 5407–5415, May 2021, doi: 10.1109/JESTPE.2020.3027864.

[16] Y. Yu et al., "Full parameter estimation for permanent magnet synchronous motors," *IEEE Trans. Ind. Electron.*, vol. 69, no. 5, pp. 4376–4386, May 2022, doi: 10.1109/TIE.2021.3078391.

[17] A. Brosch, O. Wallscheid, and J. Böcker, "Long-term memory recursive least squares online identification of highly utilized permanent magnet synchronous motors for finite-control-set model predictive control," *IEEE Trans. Power Electron.*, vol. 38, no. 2, pp. 1451–1467, Feb. 2023, doi: 10.1109/TPEL.2022.3206598.

[18] M. N. Uddin and S. W. Nam, "New online loss-minimization-based control of an induction motor drive," *IEEE Trans. Power Electron.*, vol. 23, no. 2, pp. 926–933, Feb. 2008, doi: 10.1109/TPEL.2007.915029.

[19] A. Balamurali, G. Feng, A. Kundu, H. Dhulipati, and N. C. Kar, "Noninvasive and improved torque and efficiency calculation toward current advance angle determination for maximum efficiency control of pmsm," *IEEE Trans. Transp. Electrific.*, vol. 6, no. 1, pp. 28–40, Jan. 2020, doi: 10.1109/TTE.2019.2962333.

[20] M. Li, S. Huang, X. Wu, K. Liu, X. Peng, and G. Liang, "A virtual HF signal injection based maximum efficiency per ampere tracking control for IPMSM drive," *IEEE Trans. Power Electron.*, vol. 35, no. 6, pp. 6102–6113, Jun. 2020, doi: 10.1109/TPEL.2019.2951754.

[21] J. Rodriguez et al., "Latest advances of model predictive control in electrical drives part I: Basic concepts and advanced strategies," *IEEE Trans. Power Electron.*, vol. 37, no. 4, pp. 3927–3942, Apr. 2022, doi: 10.1109/TPEL.2021.3121532.

[22] X. Li, K. Lu, Y. Zhao, D. Chen, P. Yi, and W. Hua, "Incorporating harmonic-analysis-based loss minimization into MPTC for efficiency improvement of FCFMPM motor," *IEEE Trans. Ind. Electron.*, vol. 70, no. 7, pp. 6540–6550, Jul. 2023, doi: 10.1109/TIE.2022.3201341.

[23] W. Xie, X. Wang, F. Wang, W. Xu, R. Kennel, and D. Gerling, "Dynamic loss minimization of finite control set-model predictive torque control for electric drive system," *IEEE Trans. Power Electron.*, vol. 31, no. 1, pp. 849–860, Jan. 2016, doi: 10.1109/TPEL.2015.2410427.

[24] M. Preindl and S. Bolognani, "Model predictive direct torque control with finite control set for pmsm drive systems, part 1: Maximum torque per ampere operation," *IEEE Trans. Ind. Inform.*, vol. 9, no. 4, pp. 1912–1921, Apr. 2013, doi: 10.1109/TII.2012.2227265.

[25] Z. Liu, K. Mao, X. Lei, S. Zheng, and H. Zhang, "Loss minimization control based on bivariate extreme value theory for PMSMS," *IEEE Trans. Power Electron.* vol. 39, no. 2, pp. 2004–2012, Feb. 2024, doi: 10.1109/TPEL.2023.3307237.

[26] X. Wang, Z. Zhao, K. Li, Y. Zhu, and K. Chen, "Analytical methodology for loss calculation of SiC MOSFETS," *IEEE J. Emerg. Sel.*

Topics Power Electron., vol. 7, no. 1, pp. 71–83, Jan. 2019, doi: 10.1109/JESTPE.2018.2863731.

[27] B. Stellato, T. Geyer, and P. J. Goulart, "High-speed finite control set model predictive control for power electronics," *IEEE Trans. Power Electron.*, vol. 32, no. 5, pp. 4007–4020, May 2017, doi: 10.1109/TPEL.2016.2584678.

[28] M. F. Elmorshedy, W. Xu, S. M. Allam, J. Rodriguez, and C. Garcia, "MTPA-based finite-set model predictive control without weighting factors for linear induction machine," *IEEE Trans. Ind. Electron.*, vol. 68, no. 3, pp. 2034–2047, Mar. 2021, doi: 10.1109/TIE.2020.2972432.

Sunbo Wang received the B.S. degree in electrical engineering from Beijing Institute of Technology, Beijing, China, in 2020. He is currently working toward the Ph.D. degree in electronic engineering with the Power Electronics, Machines and Control Group, University of Nottingham, Nottingham, U.K.

His research interests include control strategy of PM machines and multiphase machines, high efficiency high speed ac motor drives, and pulsewidth-modulation strategies.

Marco Rivera (Senior Member, IEEE) received the B.Sc. degree in electronic civil, the M.Sc. degree in engineering, with a specialization in electrical engineering, from the Universidad de Concepción, Concepción, Chile, and the Ph.D. degree in electronic engineering from the Universidad Técnica Federico Santa María Valparaíso, Chile.

He was awarded the "Premio Tesis de Doctorado Academia Chilena de Ciencias 2012," for the best Ph.D. Thesis developed, in 2011, for the national and the foreign students in any exact or natural sciences program, that is member of the Academia Chilena de Ciencias, Santiago, Chile. Through the last years, he has been a Visiting Professor with several international universities. He has directed and participated in several projects financed by the National Fund for Scientific and Technological Development (Fondo Nacional de Desarrollo Científico y Tecnológico, FONDECYT), the Chilean National Agency for Research and Development (Agencia Nacional de Investigación y Desarrollo, ANID), and the Paraguayan Program for the Development of Science and Technology (Proyecto Paraguayo para el Desarrollo de la Ciencia y Tecnología, PROCIENCIA), among others. He has been the responsible Researcher of basal financed projects whose objective is to enhance, through substantial and long-term financing, Chile's economic development through excellence and applied research. He is the Director of the Laboratory of Energy Conversion and Power Electronics (Laboratorio de Conversión de Energías y Electrónica de Potencia, LCEEP) with Universidad de Talca, Talca, Chile. He was a Full Professor with the Department of Electrical Engineering, Universidad de Talca. Since 2023, he has been a Pofessor with the Power Electronics, Machines and Control (PEMC) Research Institute, University of Nottingham, Nottingham, U.K. He has published more than 520 academic publications in leading international conferences and journals. His research interests include power electronics, renewable energies, advanced control of power converters, microgrids, among others.

Chris Gerada (Senior Member, IEEE) received the Ph.D. degree in numerical modeling of electrical machines from the University of Nottingham, Nottingham, U.K., in 2005.

Currently, he is an Associate Pro-Vice-Chancellor of Industrial Strategy and Impact and a Professor of electrical machines with the University of Nottingham. He has secured more than Â£20M of funding through main industrial, European, and U.K. grants. He has authored more than 350 referred publications. His research interests include electromagnetic energy conversion in electrical machines and drives, focusing mainly on transport electrification.

Prof. Gerada was awarded a Research Chair from the Royal Academy of Engineering, in 2013.

Patrick Wheeler (Fellow, IEEE) received the B.Eng. (Hons.) and the Ph.D. degrees in electrical engineering for his work on matrix converters from the University of Bristol, Bristol, U.K., in 1990 and 1994, respectively.

In 1993, he moved to the University of Nottingham and worked as a Research Assistant with the Department of Electrical and Electronic Engineering, Nottingham, U.K. In 1996, he became a Lecturer with Power Electronics, Machines and Control Group, University of Nottingham, Nottingham, U.K. Since 2008, he has been a Full Professor with the same research group. He is currently the Global Engagement Director of the Faculty of Engineering, the Head of the Power Electronics, Machines and Control Research Group, and the Director of the University of Nottingham's Institute of Aerosapce Technology. He was the Head of the Department of Electrical and Electronic Engineering, University of Nottingham, from 2015 to 2018. He has authored or co-authored more than 850 academic publications in leading international conferences and journals.

Dr. Wheeler is a member of the IEEE PELS ADCOM and is currently IEEE PELS Vice-President of Technical Operations.

Neophytos Lophitis received the B.A., M.Eng., and the Ph.D. degrees in power devices from the University of Cambridge, Cambridge, U.K., in 2008, 2009, and 2014, respectively.

He was a Consultant for Cambridge Microelectronics Ltd., Cambridge, UK, from 2013 to 2015, and a Research Associate in power with the University of Cambridge, from 2014 to 2015. In 2015, he joined Coventry University, Coventry, U.K., where he is currently an Assistant Professor of electrical engineering with the School of Computing, Electronics and Mathematics, University of Coventry, Coventry, UK, and the Research Institute for Future Transport and Cities, University of Coventry.